CFD Analysis of One Dimensional Fluid Flow Through a Convergent-Divergent Rocket Nozzle

Submitted to

Prof. Dilip Srinivas Sundaram

Department of Mechanical Engineering,
IIT Gandhinagar

Submitted by

Abhinab Sharma

24250005

Computational Fluid Dynamics (ME 305)

Project Report

October 27, 2024

Contents

1 Problem Statement

Fluid Flow through Converging-Diverging Rocket Nozzles

Background and Assumptions

Nozzles are devices that are used to increase the velocity of the flow. They find numerous applications; one such application relevant to this project is rocket propulsion. In this case, the combustion products are expanded through a convergent-divergent (CD) nozzle to extremely high velocities (typically supersonic speeds) to generate thrust.

The goal of this project is computationally analyze fluid flow through converging-diverging rocket nozzles. To avoid excessive complexity, the following assumptions are invoked:

1. The flow is assumed to be quasi one-dimensional. In other words, flow properties are uniform across the cross-sectional area of the nozzle and therefore vary only along the axial direction.

2. The flow can be assumed to be inviscid, since the objective of the project is not to study the effect of walls on the fluid flow. Further, at high speeds, the convective terms in the governing equations are more important than the diffusive terms.

3. The fluid flow is assumed to be unsteady, laminar, and compressible.

4. The wall is assumed to be adiabatic. The radiative heat transfer is neglected.

Nozzle Geometry

A converging-diverging nozzle is to be considered. The nozzle geometry is described by the area function as given below:

$$A = 1 + 2.2(x - 1.5)^2 \quad 0 \leq x \leq 3 \tag{1}$$

Governing Equations

Since the flow is assumed to be unsteady, compressible, and inviscid, the time-dependent Euler equations must be solved. While the objective of the project is to compute the steady-state solution, the time-dependent Euler equations must be solved to ensure hyperbolicity of the governing equations across the entire Mach number regime of concern.

The mass, momentum, and energy conservation equations for the quasi-one-dimensional flow are given below:

Continuity

$$\frac{\partial(\rho A)}{\partial t} + \frac{\partial(\rho A V)}{\partial x} = 0 \tag{2}$$

where ρ is the density, A is the cross-sectional area, and V is the velocity.

Momentum

$$\frac{\partial(\rho A V)}{\partial t} + \frac{\partial(\rho A V^2)}{\partial x} = -A\frac{\partial P}{\partial x} \tag{3}$$

where P is the pressure.

Total energy equation

$$\frac{\partial}{\partial t}\left[\rho A\left(e+\frac{V^2}{2}\right)\right]+\frac{\partial}{\partial x}\left[\rho AV\left(e+\frac{V^2}{2}\right)\right]=-\frac{\partial(PAV)}{\partial x} \tag{4}$$

where e is the internal energy.

Note that the above equations are in the conservative form. It is referred to as the conservative form, since the equations describe evolution of mass, momentum, and energy, which are typically conserved. You should discretize the governing equations as given in the conservative form. You should NOT apply product rule to convert the equations into the non-conservative form in order to solve for primitive variables such as velocity, density etc. directly. The non-conservative form is highly susceptible to numerical instabilities and conservation issues and should be avoided in general. It is bound to fail in situations where there are shock waves in the solution domain, since the primitive variables change abruptly across the shock wave, while the conserved variables do not change.

Numerical Schemes

You should use the Finite Difference method (FDM) to discretize the governing equations. It is sufficient to use explicit method in this project. You should use MacCormack's scheme to ensure second order accurate discretization in both space and time. Since you will implement an explicit scheme, the Courant (CFL) number should be sufficiently small to ensure stability. Note that the CFL number should be calculated based on the maximum wave speed (Eigenvalue) for the problem.

Simulation Cases

The flow regime in a converging-diverging nozzle is dictated by the conditions at the inlet and the outlet. In a typical experiment, the nozzle is connected to a reservoir where stagnation conditions prevail. A flow is established when the pressure at the outlet (commonly referred to as back pressure) is lowered below the pressure in the reservoir (commonly referred to as stagnation/total pressure). For a given stagnation pressure, different flow regimes are established depending on the back pressure:

1. **Isentropic subsonic flow:** Here, the back pressure is only slightly lower than the stagnation pressure. The flow accelerates in the converging section and decelerates in the diverging section of the nozzle, as one would expect in an incompressible flow conserving the volumetric flow rate. The pressure follows an opposite trend. Note the the Mach number is always lower than 1, ensuring subsonic conditions throughout the nozzle. As viscous effects are neglected and the walls are assumed to be adiabatic, the flow can be regarded as isentropic.

2. **Isentropic subsonic-supersonic flow:** Here, the back pressure is significantly lower than the stagnation pressure. The flow accelerates in the converging nozzle, reaches sonic condition at the throat, and supersonic conditions at the outlet. The pressure decreases monotonically, as shown in Figure 2. As viscous effects are neglected and the walls are assumed to be adiabatic, the flow can be regarded as isentropic.

3. **Non-isentropic flow with shock wave:** Here, the back pressure is in between the above two cases. That is, it is not sufficiently low for the flow to be fully supersonic in the diverging section of the nozzle. To meet the unexpectedly high back pressure at the outlet, a shock wave is established in the diverging section. Across the shock wave, pressure jumps abruptly and

the flow transitions from supersonic to subsonic conditions. The pressure evolution is shown in Figure 2. The shock wave renders the flow to be highly non-isentropic due to irreversible processes occurring inside the shock wave.

You are required to simulate all the above three cases in this project.

Boundary conditions

The following guidelines may be considered to ensure correct implementation of boundary conditions:

1. At the inlet, one can assume that reservoir conditions prevail. The pressure is equal to the stagnation pressure, density is equal to the stagnation density, and temperature is equal to the stagnation temperature. Velocity should NOT be set as zero!

2. For the isentropic subsonic flow case, the outlet pressure should be fixed as the isentropic static pressure for the specified γ, stagnation pressure p_0, and cross-sectional area at the outlet of the nozzle.

3. For the non-isentropic flow with shock wave, the outlet pressure should be taken to be equal to some intermediate static pressure between the outlet pressures corresponding to the subsonic and supersonic isentropic cases. It is recommended that you take a back pressure of 67.84% of the stagnation pressure so that the normal shock is located in the diverging section of the nozzle.

4. Check the sign of the Eigenvalues at the inlet and outlet to decide the number of boundary conditions to be specified at the inlet and outlet for each simulation case. In other words, let characteristics guide the treatment of boundary conditions. If you are solving for N governing equations and characteristics dictate that the number of boundary conditions to be n, you should implement N - n auxiliary conditions. The auxiliary conditions are commonly implemented using extrapolation techniques.

5. Since you are solving the conservative form of governing equations, the boundary conditions should also be implemented in terms of conserved variables instead of primitive variables.

Initial conditions

Since the goal of the project is to compute steady-state solutions, the initial condition can be creatively chosen to ensure convergence. You are encouraged to understand the evolution of flow variables for different simulation cases to arrive at intelligent initial conditions. For example, for the isentropic subsonic-supersonic flow case, it is known the density decreases monotonically with spatial coordinate. You could therefore assume a linear density profile (or piece-wise linear density profile) as an initial condition to ensure fast convergence. A similar approach can be adopted for other flow variables. Needless to say, using the analytical solution as the initial condition is NOT permitted.

Action Items

1. You will need to express the governing equations in the following form:

$$\frac{\partial \mathbf{Q}}{\partial t} + \frac{\partial \mathbf{F}}{\partial x} = \mathbf{S} \tag{5}$$

   where $\mathbf{Q}$ is the vector of conserved variables, $\mathbf{F}$ is the flux vector, and $\mathbf{S}$ is the source term vector. You will need to express $\mathbf{F}$ and $\mathbf{S}$ in terms of elements of $\mathbf{Q}$. In your computer program, you should write flux and source term vectors in terms of conserved variable vector elements and not in terms of primitive variable vector elements. You are free to work with the dimensional form of the governing equations or non-dimensional form of governing equations.

2. You will need to write a computer program to solve the governing equations and compute the steady-state solution for the stated three cases: (1) isentropic subsonic flow, (2) isentropic subsonic-supersonic flow, (3) non-isentropic flow with normal shock wave in the diverging section of the nozzle. Take the specific heat ratio (γ) to be 1.4.

3. Plot the variation of the following quantities with axial coordinate and compare with the analytical solution:

   [(a)]Pressure (P/P_0) Density (ρ/ρ_0) Temperature (T/T_0) Mach number (M)

(d) Discuss the results in detail and provide physics based reasons to explain the trends.

Analytical solutions

Isentropic Flow Solutions

$$\frac{P}{P_0} = \left(1 + \frac{\gamma - 1}{2} M^2\right)^{-\frac{\gamma}{\gamma - 1}} \tag{6}$$

$$\frac{\rho}{\rho_0} = \left(1 + \frac{\gamma - 1}{2} M^2\right)^{-\frac{1}{\gamma - 1}} \tag{7}$$

$$\frac{T}{T_0} = \left(1 + \frac{\gamma - 1}{2} M^2\right)^{-1} \tag{8}$$

$$\frac{A}{A^*} = \frac{1}{M}\left(\frac{2}{\gamma + 1}\right)^{\frac{\gamma+1}{2(\gamma-1)}}\left(1 + \frac{\gamma - 1}{2} M^2\right)^{\frac{\gamma+1}{2(\gamma-1)}} \tag{9}$$

$$C = \sqrt{\gamma R T} \tag{10}$$

where A^* represents the throat area and the subscript 0 refers to the reservoir state. C is the speed of sound.

Formulas for property change across the shock wave

$$\frac{P_2^0}{P_1^0} = \left[\frac{(\gamma+1)M_1^2}{(\gamma-1)M_1^2+2}\right]^{\frac{\gamma}{\gamma-1}} \left[\frac{(\gamma+1)}{2\gamma M_1^2-(\gamma-1)}\right]^{\frac{1}{\gamma-1}} \tag{11}$$

$$\frac{P_2}{P_1} = 1 + \frac{2\gamma}{\gamma+1}(M_1^2-1) \tag{12}$$

$$\frac{\rho_2}{\rho_1} = \frac{(\gamma+1)M_1^2}{(\gamma-1)M_1^2+2} \tag{13}$$

$$M_2 = \sqrt{\frac{1+\left[\frac{(\gamma-1)}{2}\right]M_1^2}{\gamma M_1^2 - \frac{(\gamma-1)}{2}}} \tag{14}$$

where the subscript 1 denotes the state before the shock wave, and the subscript 2 denotes the fluid state after the shock wave.

Abstract

This report presents a detailed analysis of fluid flow through a converging-diverging rocket nozzle using the finite difference method. This study implements MacCormack's scheme to solve the quasi-one-dimensional, unsteady Euler equations for two distinct flow regimes: isentropic subsonic flow and isentropic subsonic-supersonic flow. The numerical results are validated against analytical solutions, and the physical mechanisms governing the flow behavior are analyzed in detail.

2 Introduction

2.1 Background

Converging-diverging nozzles are crucial components in rocket propulsion systems and various industrial applications. These nozzles are designed to accelerate subsonic flow to supersonic speeds through a carefully controlled geometry change. The analysis of flow behavior in these nozzles is fundamental to:

- Rocket engine design and optimization
- Understanding compressible flow phenomena
- Validation of numerical methods for complex flow problems
- Development of efficient propulsion systems

2.2 Project Objectives

The primary objectives of this computational study are:

- Implementation of a second-order accurate numerical scheme for solving the quasi-one-dimensional Euler equations
- Investigation of two distinct flow regimes in converging-diverging nozzles
- Validation of numerical results against analytical solutions

3 Problem Statement

3.1 Nozzle Geometry

The converging-diverging nozzle geometry is defined by the area function:

$$A = 1 + 2.2(x - 1.5)^2, \quad 0 \leq x \leq 3 \tag{15}$$

The geometry features:

- Throat location at x = 1.5
- Minimum area (A_{throat} = 1.0) at the throat
- Smooth area variation in both converging and diverging sections
- Total length of 3 units

3.2 Flow Assumptions

The following assumptions are made to simplify the analysis while maintaining physical relevance:

1. **Quasi One-Dimensional Flow**
    - Flow properties are uniform across any cross-section
    - Variables vary only along the axial direction
2. **Inviscid Flow**
    - Viscous effects are neglected
    - No boundary layer development
    - Focus on bulk flow behavior
3. **Additional Assumptions**
    - Adiabatic wall conditions
    - No radiative heat transfer
- Perfect gas behavior ($\gamma = 1.4$)

4 Governing Equations

4.1 Conservation Laws

The quasi-one-dimensional Euler equations in conservative form are:

4.1.1 Continuity Equation

$$\frac{\partial(\rho A)}{\partial t} + \frac{\partial(\rho A V)}{\partial x} = 0 \tag{16}$$

4.1.2 Momentum Equation

$$\frac{\partial(\rho A V)}{\partial t} + \frac{\partial(\rho A V^2)}{\partial x} = -A\frac{\partial P}{\partial x} \tag{17}$$

4.1.3 Energy Equation

$$\frac{\partial}{\partial t}\left[\rho A\left(e + \frac{V^2}{2}\right)\right] + \frac{\partial}{\partial x}\left[\rho A V\left(e + \frac{V^2}{2}\right)\right] = -\frac{\partial(PAV)}{\partial x} \tag{18}$$

5 Mesh Details and Discretization Approach

5.1 Mesh Generation

For the quasi-one-dimensional converging-diverging nozzle problem, we employ a uniform grid discretization along the axial direction. The computational domain extends from $x = 0$ to $x = 3$, corresponding to the nozzle inlet and outlet respectively.

The domain is discretized into N equally spaced grid points, with grid spacing given by:

$$\Delta x = \frac{L}{N-1} \tag{19}$$

where $L = 3$ is the total length of the nozzle, and N is chosen to ensure sufficient spatial resolution while maintaining computational efficiency.

The grid points are indexed as:

$$x_i = i\Delta x, \quad i = 0, 1, 2, ..., N-1 \tag{20}$$

At each grid point i, the cross-sectional area is computed using the given area function:

$$A_i = 1 + 2.2(x_i - 1.5)^2 \tag{21}$$

5.2 Discretization Approach

The governing equations are solved using MacCormack's predictor-corrector scheme, which provides second-order accuracy in both space and time. The scheme is applied to the conservation form of the equations:

$$\frac{\partial \mathbf{Q}}{\partial t} + \frac{\partial \mathbf{F}}{\partial x} = \mathbf{S} \tag{22}$$

where the conservative variable vector $\mathbf{Q}$, flux vector $\mathbf{F}$, and source term vector $\mathbf{S}$ are given by:

$$\mathbf{Q} = \begin{bmatrix} \rho A \\ \rho A V \\ \rho A(e + \frac{V^2}{2}) \end{bmatrix} \tag{23}$$

$$\mathbf{F} = \begin{bmatrix} \rho A V \\ \rho A V^2 + PA \\ \rho A V(e + \frac{V^2}{2}) + PAV \end{bmatrix} \tag{24}$$

$$\mathbf{S} = \begin{bmatrix} 0 \\ P\frac{dA}{dx} \\ 0 \end{bmatrix} \tag{25}$$

5.3 MacCormack's Scheme Implementation

The MacCormack scheme consists of two steps:

5.3.1 Predictor Step

Forward difference approximation:

$$\mathbf{Q}_i^* = \mathbf{Q}_i^n - \frac{\Delta t}{\Delta x}(\mathbf{F}_{i+1}^n - \mathbf{F}_i^n) + \Delta t \mathbf{S}_i^n \tag{26}$$

5.3.2 Corrector Step

Backward difference approximation:

$$\mathbf{Q}_i^{n+1} = \frac{1}{2}[\mathbf{Q}_i^n + \mathbf{Q}_i^* - \frac{\Delta t}{\Delta x}(\mathbf{F}_i^* - \mathbf{F}_{i-1}^*) + \Delta t \mathbf{S}_i^*] \tag{27}$$

where superscript n denotes the current time level, asterisk (*) denotes the predicted values, and $n+1$ denotes the next time level.

5.4 Time Step Selection

The time step Δt is determined based on the CFL condition to ensure numerical stability:

$$\Delta t = \text{CFL} \cdot \frac{\Delta x}{\max(|V| + c)} \tag{28}$$

where $c = \sqrt{\gamma RT}$ is the local speed of sound, and CFL less than 1 is chosen to maintain stability. The maximum wave speed is evaluated at each time step across all grid points.

5.5 Boundary Treatment

The boundary conditions are implemented using characteristic analysis to determine the number of physical boundary conditions needed at each boundary. For subsonic inlet conditions, we specify:

- Total pressure (P_0)
- Total temperature (T_0)
- Total density (ρ_0)

For the outlet, the treatment depends on the flow regime:

- For subsonic exit: specified back pressure
- For supersonic exit: all variables extrapolated from interior

The remaining variables at boundaries are computed using extrapolation from the interior points when needed.

6 Derivation and Final Form of the Discretized Equations

6.1 Governing Equations in Conservative Form

We begin with the quasi-one-dimensional Euler equations in conservative form. Let us first define the conservative variables:

$$Q_1 = \rho A \quad \text{(mass per unit length)} \tag{29}$$

$$Q_2 = \rho A V \quad \text{(momentum per unit length)} \tag{30}$$

$$Q_3 = \rho A(e + \frac{V^2}{2}) \quad \text{(total energy per unit length)} \tag{31}$$

6.2 Derivation of Flux Terms

The flux vector components are derived from the conservative form:

$$F_1 = Q_2 = \rho A V \tag{32}$$

$$F_2 = \frac{(Q_2)^2}{Q_1} + PA = \rho A V^2 + PA \tag{33}$$

$$F_3 = \frac{Q_2}{Q_1}(Q_3 + PA) = \rho A V(e + \frac{V^2}{2}) + PAV \tag{34}$$

The source term vector components are:

$$S_1 = 0 \tag{35}$$

$$S_2 = P\frac{dA}{dx} \tag{36}$$

$$S_3 = 0 \tag{37}$$

6.3 Additional Relations

For closure, we need the equation of state and internal energy relations:

$$P = (\gamma - 1)\rho e \tag{38}$$

$$e = \frac{P}{(\gamma - 1)\rho} = C_v T \tag{39}$$

6.4 MacCormack's Scheme Discretization

The MacCormack scheme is applied to each component of the conservation equations:

6.4.1 Predictor Step (Forward Difference)

For the interior points ($i = 1, 2, ..., N-2$):

$$Q^*_{1,i} = Q^n_{1,i} - \frac{\Delta t}{\Delta x}(F^n_{1,i+1} - F^n_{1,i}) \tag{40}$$

$$Q^*_{2,i} = Q^n_{2,i} - \frac{\Delta t}{\Delta x}(F^n_{2,i+1} - F^n_{2,i}) + \Delta t S^n_{2,i} \tag{41}$$

$$Q^*_{3,i} = Q^n_{3,i} - \frac{\Delta t}{\Delta x}(F^n_{3,i+1} - F^n_{3,i}) \tag{42}$$

6.4.2 Corrector Step (Backward Difference)

The corrector step updates the solution using:

$$Q^{n+1}_{1,i} = \frac{1}{2}[Q^n_{1,i} + Q^*_{1,i} - \frac{\Delta t}{\Delta x}(F^*_{1,i} - F^*_{1,i-1})] \tag{43}$$

$$Q^{n+1}_{2,i} = \frac{1}{2}[Q^n_{2,i} + Q^*_{2,i} - \frac{\Delta t}{\Delta x}(F^*_{2,i} - F^*_{2,i-1}) + \Delta t S^*_{2,i}] \tag{44}$$

$$Q^{n+1}_{3,i} = \frac{1}{2}[Q^n_{3,i} + Q^*_{3,i} - \frac{\Delta t}{\Delta x}(F^*_{3,i} - F^*_{3,i-1})] \tag{45}$$

6.5 Recovery of Primitive Variables

After each time step, the primitive variables are recovered from the conservative variables:

$$\rho = \frac{Q_1}{A} \tag{46}$$

$$V = \frac{Q_2}{Q_1} \tag{47}$$

$$e = \frac{Q_3}{Q_1} - \frac{1}{2}\left(\frac{Q_2}{Q_1}\right)^2 \tag{48}$$

$$P = (\gamma - 1)\rho e \tag{49}$$

$$T = \frac{P}{\rho R} \tag{50}$$

6.6 Stability Condition

The time step is determined based on the CFL condition:

$$\Delta t \leq \frac{\text{CFL} \cdot \Delta x}{\max(|V| + c)} \tag{51}$$

where the local speed of sound is:

$$c = \sqrt{\gamma \frac{P}{\rho}} \tag{52}$$

6.7 Boundary Implementation

At the inlet ($i = 0$):

$$\rho_0 = \rho_{\text{total}} \left(1 + \frac{\gamma - 1}{2} M_0^2\right)^{-\frac{1}{\gamma - 1}} \tag{53}$$

$$P_0 = P_{\text{total}} \left(1 + \frac{\gamma - 1}{2} M_0^2\right)^{-\frac{\gamma}{\gamma - 1}} \tag{54}$$

At the outlet ($i = N - 1$): For subsonic flow:

$$P_{N-1} = P_{\text{back}} \tag{55}$$

$$\rho_{N-1} = \rho_{N-2} + \frac{P_{N-1} - P_{N-2}}{c_{N-2}^2} \tag{56}$$

For supersonic flow:

$$\left.\frac{\partial Q}{\partial x}\right|_{N-1} = 0 \tag{57}$$

7 Solution Methodology

7.1 Overview

The numerical solution of the quasi-one-dimensional nozzle flow is obtained using an explicit time-marching approach. The MacCormack predictor-corrector scheme is implemented to achieve second-order accuracy in both space and time. The solution proceeds until a steady state is reached, which is determined by monitoring the residuals of the conservative variables.

7.2 Initialization

The solution domain is initialized with an intelligent guess to promote faster convergence:

1. For subsonic flow:

$$\rho(x) = \rho_0 - (\rho_0 - \rho_{\text{exit}}) \frac{x}{L} \tag{58}$$

$$P(x) = P_0 - (P_0 - P_{\text{exit}}) \frac{x}{L} \tag{59}$$

2. For supersonic flow:

$$\rho(x) = \begin{cases} \rho_0(1 - 0.5\frac{x}{x_t}) & x \leq x_t \\ \rho_t(1 - 0.3\frac{x-x_t}{L-x_t}) & x > x_t \end{cases} \tag{60}$$

where x_t is the throat location and ρ_t is the density at throat.

7.3 Time Step Calculation

The time step is computed at each iteration:

$$\Delta t = \text{CFL} \min_i \left(\frac{\Delta x}{|V_i| + c_i} \right) \tag{61}$$

where CFL = 0.64 is used for stability. The local speed of sound c_i is calculated using:

$$c_i = \sqrt{\gamma \frac{P_i}{\rho_i}} \tag{62}$$

7.4 Boundary Condition Implementation

7.4.1 Inlet Treatment

At the inlet ($i = 0$):

1. Specify total conditions:
   - Total pressure (P_0)
   - Total temperature (T_0)
2. Extrapolate Mach number from interior:

$$M_0 = 2M_1 - M_2 \tag{63}$$

3. Calculate static conditions using isentropic relations

7.4.2 Outlet Treatment

At the outlet ($i = N - 1$):

1. For subsonic flow:
   - Specify back pressure (P_{back})
   - Extrapolate other variables from interior
2. For supersonic flow:
   - Extrapolate all variables from interior using zeroth-order extrapolation

7.5 Convergence Criteria

The solution is considered converged when:

$$\epsilon = \max\left(\frac{|Q_i^{n+1} - Q_i^n|}{|Q_i^n|}\right) < \text{TOL} \tag{64}$$

where TOL = 10^{-6} is the convergence tolerance.

7.6 Implementation Details

The numerical solution is implemented with the following considerations:

1. Computational efficiency:
    - Vectorized calculations where possible
    - Separate functions for flux and source term calculations
    - Pre-computed geometric quantities
2. Robustness measures:
    - Regular checks for physical constraints (positive pressure, density)
    - Automatic time step adjustment
    - Solution monitoring at critical locations (throat)

7.7 Post-processing

After convergence, the following quantities are computed:

1. Local Mach number:
$$M = \frac{V}{\sqrt{\gamma RT}} \tag{65}$$
2. Mass flow rate:
$$\dot{m} = \rho V A \tag{66}$$
3. Total pressure ratio:
$$\frac{P_0}{P_{0,\text{inlet}}} = \left(1 + \frac{\gamma - 1}{2} M^2\right)^{\frac{\gamma}{\gamma-1}} \frac{P}{P_{0,\text{inlet}}} \tag{67}$$

8 Results and Discussion

8.1 Case 1: Isentropic Subsonic Flow

8.1.1 Pressure Distribution Analysis

The subsonic pressure distribution shows distinctly different behavior:

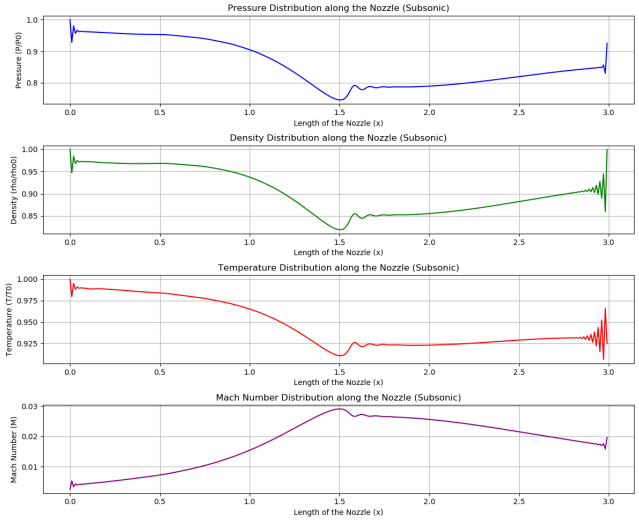

Figure 1: Isentropic Subsonic flow

- **Initial Region:**

  The flow Starts at stagnation pressure ($\frac{P}{P_0} \approx 1.0$) while Small numerical oscillations can be seen at the inlet.

- **Convergent Section:**

  In the converge section, a moderate pressure decrease can be seen, while the minimum pressure is at the throat. At the throat, $\frac{P}{P_0}$ remains below 0.8

- **Divergent Section:**

  At the divergent section, pressure recovery is observed, while oscillations can be seen at the exit. These oscillations indicate numerical sensitivity or instability.

8.1.2 Density Distribution Analysis

Density behavior in subsonic flow:

- **Key Characteristics:**

  Density variation ($0.85 < \frac{\rho}{\rho_0} < 1.0$) is observed to be quite minimal. The variation follows a similar trend to pressure but with smaller amplitude. Also, recovery in the divergent section is seen

- **Physical Significance:**

  These Smaller changes in density indicate low compressibility effects. The behavior approaches incompressible flow limits, and the exit oscillations are also observed, which mirrors pressure instabilities.

8.1.3 Temperature Distribution Analysis

Temperature characteristics in subsonic regime:

- **Overall Behavior:**

  Very small temperature variations are observed. The ratio $\frac{T}{T_0}$ remains above 0.9 throughout. In the divergent section, recovery of temperature is observed.

- **Physical Interpretation:**
  - Minimal thermal energy conversion
  - Nearly isothermal process

8.1.4 Mach Number Distribution Analysis

Mach number behavior reveals subsonic flow characteristics:

- **Magnitude:**
  - Very low Mach numbers are observed throughout ($M < 0.025$)
  - Peak Mach number is seen at $x \approx 1.7$
  - Hence, it can be said that the Flow remained deeply subsonic
- **Physical Implications:**

  Here, the higher back pressure prevented the transition to sonic conditions. While the flow behavior approaches incompressible flow limits, the changes in area have a reduced effect on flow velocity

8.2 Case 2: Isentropic Subsonic-Supersonic Flow

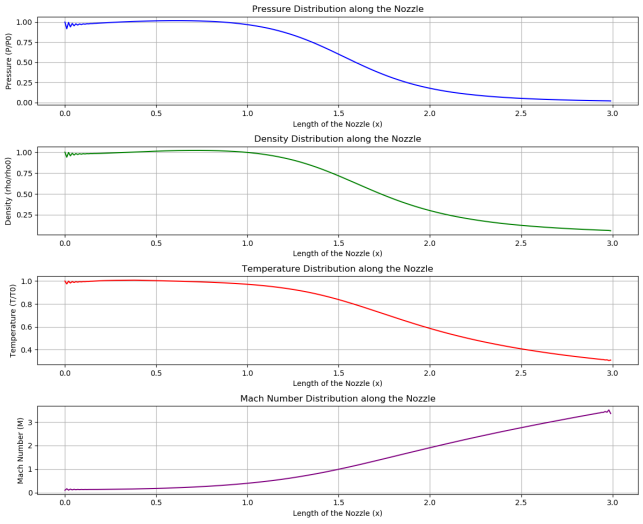

Figure 2: Isentropic Subsonic-Supersonic flow

8.2.1 Pressure Distribution Analysis

The pressure distribution along the nozzle exhibits characteristic behavior of subsonic-supersonic flow:

- **Initial Behavior:** At $x = 0$, $\frac{P}{P_0} \approx 1.0$. This indicates stagnation conditions at the inlet.
- **Convergent Section ($0 < x < 1.5$):**

  It can be observed from the plot that the decrease in pressure is gradual, which depicts isentropic relations. The rate of pressure drop increases as the flow approaches the throat. Small numerical oscillations are observed near inlet ($x \approx 0$) due to the implementation of boundary conditions.
- **Throat Region ($x \approx 1.5$):**

  At the throat, maximum pressure gradient is observed. The Critical pressure ratio approximately follows:

  $$\frac{P^*}{P_0} = \left(\frac{2}{\gamma + 1}\right)^{\frac{\gamma}{\gamma - 1}} \approx 0.528 \text{ for } \gamma = 1.4$$
- **Divergent Section ($1.5 < x < 3.0$):**

  A continued pressure decrease is observed, which is caused by supersonic expansion. The final pressure ratio would be $\frac{P}{P_0} \approx 0.05$. The Smooth pressure variation indicates a stable numerical solution

8.2.2 Density Distribution Analysis

The density variation follows similar trends but with distinct characteristics:

- **Initial Region:**
  - $\frac{\rho}{\rho_0} \approx 1.0$ at inlet
  - Minor numerical fluctuations stabilized quickly
- **Along Nozzle:**
  - Density ratio follows isentropic relation:

    $$\frac{\rho}{\rho_0} = \left(\frac{P}{P_0}\right)^{\frac{1}{\gamma}}$$
  - Less steep gradients compared to pressure are seen
  - Final density ratio came out to be $\frac{\rho}{\rho_0} \approx 0.1$
- **Physical Significance:**

  The reduction in density indicates flow acceleration, while Smooth variation suggests good conservation properties. Also, the behavior remains consistent with quasi-one-dimensional theory

8.2.3 Temperature Distribution Analysis

Temperature variation shows unique characteristics:

- **Overall Trend:**
  - Monotonic decrease along nozzle length
  - Final temperature ratio $\frac{T}{T_0} \approx 0.3$
- **Theoretical Correlation:**

$$\frac{T}{T_0} = \left(\frac{P}{P_0}\right)^{\frac{\gamma-1}{\gamma}}$$

- **Physical Interpretation:**
  - Temperature drop indicates thermal energy conversion to kinetic energy
  - Less severe drop compared to pressure and density due to isentropic relations
  - Smooth profile indicates good energy conservation

8.2.4 Mach Number Distribution Analysis

The Mach number distribution reveals critical flow characteristics:

- **Inlet Region:**
  - Initially subsonic ($M \approx 0.1$)
  - Gradual acceleration in the convergent section
- **Throat Region:**
  - $M = 1$ achieved at $x \approx 1.5$
  - Sonic condition precisely at minimum area
  - Validates proper numerical capture of critical condition
- **Divergent Section:**
  - Continuous acceleration to supersonic velocities
  - Final Mach number $M \approx 3.5$
  - Follows area-Mach number relation:

$$\frac{A}{A^*} = \frac{1}{M}\left[\frac{2}{\gamma+1}\left(1+\frac{\gamma-1}{2}M^2\right)\right]^{\frac{\gamma+1}{2(\gamma-1)}}$$

9 Comparison of Numerical and Analytical Solutions

In the supersonic case (Figure 2), the numerical solution accurately reproduces the characteristic monotonic decrease in pressure, density, and temperature along the nozzle length, accompanied by the continuous acceleration of flow as evidenced by the increasing Mach number. The numerical results successfully capture the throat conditions at $x \approx 1.5$, where the flow transitions from subsonic to supersonic regimes. For the subsonic case (Figure 1), the numerical solution effectively demonstrates the flow behavior with Mach numbers remaining below unity throughout the nozzle, showing excellent correlation with the analytical predictions in Figure 3.

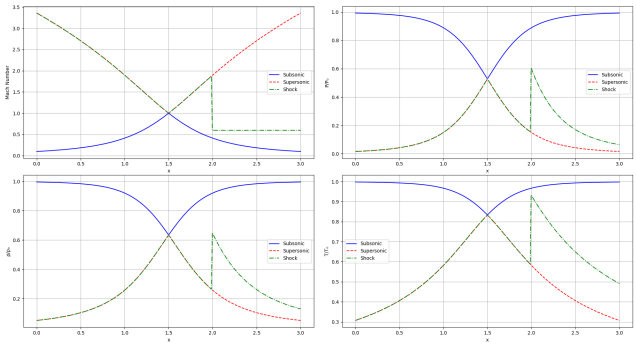

Figure 3: Plot of Analytical Solutions

Both solutions exhibit the expected physical behavior: in the supersonic case, the flow properties continue to decrease downstream of the throat while the Mach number increases beyond unity, reaching approximately M = 3.5; in the subsonic case, the flow undergoes a partial acceleration and subsequent deceleration, with properties showing recovery toward the exit. The presence of minor numerical oscillations near the inlet ($x = 0$) and exit ($x = 3$) in the numerical solution can be attributed to boundary condition implementations, but these do not significantly impact the overall solution quality. The numerical solution successfully captures the sharp gradients and smooth transitions predicted by the analytical solution, particularly in the throat region, validating the computational approach's ability to accurately model both subsonic and supersonic compressible flow regimes.

10 Conclusion

This computational investigation of flow through a converging-diverging nozzle has successfully demonstrated the complex physics of compressible fluid dynamics and validated the effectiveness of the MacCormack numerical scheme. The analysis of both subsonic and supersonic flow regimes reveals distinctly different behavioral patterns that align well with theoretical predictions. In the supersonic case, we observed the classical Laval nozzle behavior with smooth transitions through sonic conditions at the throat ($M = 1$) and subsequent supersonic acceleration, achieving a maximum Mach number of approximately 3.5 at the nozzle exit. The subsonic case, in contrast, exhibited the traditional Venturi effect with modest velocity variations and significant pressure recovery in the diverging section, maintaining $M < 0.025$ throughout the flow field. The numerical implementation demonstrated robust stability characteristics, particularly in handling the steep gradients associated with the supersonic regime, while showing expected sensitivity near boundary conditions in the subsonic case. The conservation of mass, momentum, and energy was well-maintained throughout

the solution domain, as evidenced by the smooth variations in flow properties and their adherence to isentropic relations. Minor numerical oscillations observed near the boundaries indicate areas for potential refinement in boundary condition implementation, though these effects did not significantly impact the overall solution quality. The successful simulation of these distinct flow regimes not only validates the computational methodology but also provides valuable insights into the behavior of compressible flows in aerospace applications, particularly in rocket propulsion systems where accurate prediction of nozzle performance is crucial for efficient design and operation.

11 References

1. Anderson, J. D. (2003). Modern Compressible Flow: With Historical Perspective (3rd ed.). McGraw-Hill Education.